



Published in final edited form as:

Cell. 2014 May 22; 157(5): 1146–1159. doi:10.1016/j.cell.2014.03.045.

Mechanical feedback through E-cadherin promotes direction sensing during collective cell migration

Danfeng Cai^{1,2}, Shann-Ching Chen^{3,4,*}, Mohit Prasad^{1,5,*}, Li He^{1,6}, Xiaobo Wang^{1,7}, Valerie Choesmel-Cadamuro⁷, Jessica K. Sawyer^{1,8}, Gaudenz Danuser^{3,9}, and Denise J. Montell^{1,2,#}

¹Department of Biological Chemistry, Johns Hopkins School of Medicine Baltimore, MD 21205, USA

²Molecular, Cellular and Developmental Biology Department University of California, Santa Barbara, CA 93106-9625, USA

³Department of Cell Biology, The Scripps Research Institute, La Jolla, CA 92037-1000, USA

Summary

E-cadherin is a major homophilic cell-cell adhesion molecule that inhibits motility of individual cells on matrix. However its contribution to migration of cells through cell-rich tissues is less clear. We developed an *in vivo* sensor of mechanical tension across E-cadherin molecules, which we combined with cell-type-specific RNAi, photo-activatable Rac, and morphodynamic profiling, to interrogate how E-cadherin contributes to collective migration of cells between other cells. Using the *Drosophila* ovary as a model, we found that adhesion between border cells and their substrate, the nurse cells, functions in a positive feedback loop with Rac and actin assembly to stabilize forward-directed protrusion and directionally persistent movement. Adhesion between individual border cells communicates direction from the lead cell to the followers. Adhesion between motile cells and polar cells holds the cluster together and polarizes each individual cell. Thus, E-cadherin is an integral component of the guidance mechanisms that orchestrate collective chemotaxis *in vivo*.

© 2014 Elsevier Inc. All rights reserved.

#Correspondence: denise.montell@lifesci.ucsb.edu.

⁴present address: Life Technologies, South San Francisco, CA 94080, USA

⁵present address: Department of Biological Sciences, IISER-Kolkata, West Bengal 741252, India

⁶present address: Department of Genetics, Harvard Medical School, Boston, MA 02115, USA

⁷present address: Université P. Sabatier Toulouse III, 31062 Toulouse cedex 9, France

⁸present address: Department of Pharmacology and Cancer Biology, Duke University School of Medicine, Durham, NC 27710, USA

⁹present address: Department of Cell Biology, UT Southwestern Medical Center, Dallas, TX 75235-5303, USA

*These authors contributed equally to this work

Publisher's Disclaimer: This is a PDF file of an unedited manuscript that has been accepted for publication. As a service to our customers we are providing this early version of the manuscript. The manuscript will undergo copyediting, typesetting, and review of the resulting proof before it is published in its final citable form. Please note that during the production process errors may be discovered which could affect the content, and all legal disclaimers that apply to the journal pertain.

Introduction

Epithelial cadherin (E-cadherin) is a major homophilic cell-cell adhesion molecule that interconnects epithelial cells (Niessen et al., 2011). Its elimination is considered essential, or even sufficient, to drive the morphological changes accompanying epithelial to mesenchymal transitions (EMTs), which convert immobile epithelial cells into migratory individual cells (Kalluri and Weinberg, 2009). However *in vivo* cell movements are diverse. Many cells within forming tissues, healing wounds, and invading tumors move in groups (Friedl and Gilmour, 2009). Such cells can retain E-cadherin expression, cell-cell adhesions, and apical-basal polarity and yet still migrate (Niewiadomska et al., 1999; Theveneau and Mayor, 2012). In addition, cells move through diverse environments, including on basement membranes, through interstitial matrices, or in between other cells, raising the question as to the function of cell-cell adhesion in general, and E-cadherin in particular, in diverse *in vivo* settings.

To address the roles for E-cadherin, we focused on the border cells in the *Drosophila* ovary, a well-studied *in vivo* model of collective cell migration (reviewed in Montell et al., 2012). Border cells move as a group in between cells called nurse cells. Here we generated flies expressing an optical sensor of mechanical tension, which we exploited together with cell type specific RNAi, photo-inhibitable Rac, and morphodynamic profiling of migration phenotypes. E-cadherin promotes this *in vivo* movement by multiple mechanisms, the combination of which, orchestrates collective direction-sensing. Of particular note, E-cadherin functions at the leading edge in a positive feedback loop with the small GTPase Rac as an integral part of the direction-sensing mechanism.

Results

Cell-type-specific RNAi of E-cadherin reveals dynamic defects in direction sensing

The *Drosophila* ovary is made up of chains of egg chambers of increasing maturity (Figure 1A). Each egg chamber contains 16 germ cells (15 nurse cells and one oocyte), surrounded by an epithelium of somatic follicle cells. At each pole a pair of polar cells secretes Unpaired (Upd), which activates JAK/STAT signaling in neighboring cells. This stimulates 4-8 cells at the anterior to extend protrusions in between the nurse cells, detach from the epithelium, and migrate as a cluster to the border of the oocyte (Montell et al., 2012) (Movie S1; Figures 1A-1C), where they form a structure required for sperm entry.

Contrary to the EMT paradigm, border cells up-regulate E-cadherin expression as they initiate migration (Niewiadomska et al., 1999; Figures 1A-1C). Polar cells express the highest level of E-cadherin; the outer, migratory border cells express less, and nurse cells express even less (Figures 1A-1C). Genetic ablation of E-cadherin from either border cells or nurse cells impedes their migration (Niewiadomska et al., 1999, Fulga and Rørth, 2002). However these analyses preceded live imaging of egg chambers (Prasad and Montell, 2007), so it was unclear what specific dynamic features of the behavior were defective, or which molecular pathways E-cadherin might interact with, if any. To analyze the dynamics of E-cadherin phenotypes we used cell-type-specific Gal4 drivers to express E-cadherin RNAi

lines and confirmed the knockdown (k.d.) in outer, migratory border cells (Figures 1D-1F), polar cells (Figures S1A-S1E'), and nurse cells (Figures S1F-S1H).

Cluster polarization and directional migration require border cell-nurse cell E-cadherin adhesion

When we knocked E-cadherin down in the outer, migratory border cells using *slboGal4*, in contrast to wild type (WT) (Figure 1G; Movie S1), directional persistence of migration was significantly reduced, clusters ended up in ectopic locations (Figures 1H and 1I; Movie S2), and the migration paths of E-cadherin knockdown clusters frequently deviated from a straight line (Figures 1J and 1K). Though the cells were still motile and remained clustered, E-cadherin k.d. reduced the average speed from 0.67 to 0.26 $\mu\text{m}/\text{min}$. The defect in direction sensing could only be detected by live imaging, but the end result (Figures 1L and 1M) phenocopied null mutant clones in fixed tissue (Niewiadomska et al., 1999, Fulga and Rørth, 2002) in that 90% of border cell clusters remained at the anterior of stage 10 egg chambers, which confirmed the effectiveness of the RNAi.

If border cell-nurse cell adhesion is required for normal direction sensing, then knocking down E-cadherin specifically in the nurse cells (Figure 2A) should cause a similar defect. Live imaging revealed that, in contrast to control clusters, which migrate along a straight path and reach the oocyte in ~4 hours (Movie S4; Figures 2C and 2D), nurse cell E-cadherin k.d. caused border cells to wander (Figures 2C). 70% of the clusters migrated around the outside of the egg chamber (Movie S5; Figure 2D), and even those that migrated between nurse cells did not sustain directed, posterior movement (Movie S6). Thus live imaging revealed that E-cadherin is required not for motility per se but to sustain movement in the correct direction.

When E-cadherin was over-expressed 6-fold in nurse cells (Figure 2B), fixed and live imaging revealed that the border cells migrated along the normal path (Figures 2C and 2D) more slowly than normal (Figure 2E), and exhibited a hyper-polarized morphology (Movie S7; Figure 2I). 76% of protrusions from border cell clusters migrating between WT nurse cells were directed toward the oocyte. This fraction increased to 86% when E-cadherin was over-expressed and decreased to 63% when E-cadherin was knocked down in the germline (Figure 2F) and 64% when it was knocked down in border cells (Figure 2F). Thus border cell-nurse cell adhesion promotes polarization of the cluster. Moreover protrusions were longer than normal when nurse cells over-expressed E-cadherin and shorter than normal upon E-cadherin k.d. (Figures 2G-2I).

Over-expression of E-cadherin in outer, migratory border cells using *slboGal4* or in polar cells using *UpdGal4* did not affect border cell migration significantly (Figure 2J), presumably because these cells already express high levels of E-cadherin and so only nurse cell E-cadherin is normally limiting.

Polar cell-border cell adhesion organizes the cluster

When E-cadherin was knocked down specifically in polar cells using *UpdGal4*, 73% of border cell clusters split apart (Figures 2K-2M; Movie S3). In principle, E-cadherin loss from the outer, migratory cells should also disrupt polar cell/border cell adhesion; however

cluster splitting was not observed either in *slboGal4* RNAi experiments (Figure 1H) or in null mutants (Niewiadomska et al., 1999). So when border cell-nurse cell adhesion is eliminated together with border cell-polar cell adhesion, mutant cells remain clustered, perhaps due to less friction between border cells and nurse cells. Clusters split when border cell-polar cell adhesion was weakened in the presence of normal border cell-nurse cell adhesion. Thus normally polar cell/border cell E-cadherin holds the cluster together.

An *in vivo* sensor for mechanical tension reveals a front/back difference in migrating border cells

The E-cadherin RNAi phenotypes suggested a role in direction sensing, however we detected no difference in E-cadherin concentration from front to back within border cell clusters (Figure 3A). To test whether there might be a difference in the strength of border cell-nurse cell adhesions at the front versus the back, we generated transgenic flies expressing an E-cadherin molecule that incorporated a recently developed tension sensor (TS) module (Grashoff et al., 2010). Originally tested in vinculin, the TS is composed of monomeric teal fluorescent protein (mTFP) fused to the N-terminus of a protein domain from spider silk that functions as a nano-spring, and Venus (A206K) fused to the C-terminus (Figure 3B). Under conditions of low tension the mTFP and Venus are close enough to undergo Förster resonance energy transfer (FRET), however when mechanical force is applied, the distance between the two fluorescent proteins increases and FRET decreases (Figure 3B). Thus the FRET signal responds to mechanical tension across the molecule. This module has been used to show that E-cadherin is under constitutive actomyosin-generated tension in cultured cells (Borghi et al., 2012). The TS module has also been validated in VE-cadherin and PECAM (Conway et al., 2013).

We used the TS to investigate possible differences in force transduced across E-cadherin molecules in migrating border cells. We expected tension to build up as a consequence of homophilic interactions between E-cadherins on neighboring cells and anchoring of the cytoplasmic domains to contractile actomyosin filaments via α - and β -catenins. Therefore, we inserted the TS module in between the trans-membrane domain and β -catenin binding site (Figure 3C). In this arrangement, FRET within the TS module should decrease where adhesion and contractile forces are strongest and FRET should increase where cell-cell adhesive links are absent and/or contractility is weak.

As a ratiometric probe, the FRET signal should be independent of local variations in protein concentration. However to control for any factor other than force that might change the FRET signal, such as variations in protein conformation, clustering, binding partners, pH, etc. we fused the TS module to the C-terminus of E-cadherin, which does not participate in force transduction (Figure 3D). Both the E-cadherin tension sensor (Cad^{TS}) and the load-insensitive control ($\text{Cad}^{\text{TS-C}}$) were functional *in vivo*, as they were able to rescue expression and localization of β -catenin (Armadillo, Arm; Figure 3E-3H) as well as the migration phenotypes of E-cadherin knock down in border cells (Figure 3I) or nurse cells (Figures 3J, S2A-2C). Neither construct perturbed border cell migration in a WT background (Figure 3I). In addition, both proteins co-localized with Arm (Figures 3K-3N).

We detected reproducible differences in FRET with the tension sensor - but not the load-insensitive control - between the front of migrating border cell clusters and the back (Figures 3O-3P). We quantified the FRET ratios by making $7\mu\text{m}^2$ sections in the front and in the back of the FRET image of the cluster. To distinguish border cell-nurse cell boundaries from nurse cell-nurse cell boundaries, we used Lifeact-RFP expressed with *slboGal4* to identify border cells specifically (Figures 3O' and 3P').

The front/back FRET ratio for the TS was consistently less than 1, indicating greater tension per molecule and/or a greater proportion of molecules under tension at the front of the cluster (0.89 ± 0.019 mean \pm SEM). For the control sensor the ratio was much closer to 1 (0.96 ± 0.013 mean \pm SEM; Figure 3Q). There was no significant difference in the number of E-cadherin molecules at the front of the cluster versus back (Figures 3A and S2D). To verify that the differences in FRET for the TS were actually reporting forces, we inhibited actomyosin contraction using a pharmacological inhibitor of Rho kinase, Y-27632, which we previously showed inhibits myosin activity in follicle cells (He et al, 2010). This treatment resulted in the expected FRET increase in both the front and the back of the cluster, reflecting decreased force (Figures S2G and S2H). We then treated with ionomycin, a Ca^{2+} ionophore that hyperactivates myosin in follicle cells (He et al, 2010). The Ca^{2+} biosensor GCaMP5 verified the rise in Ca^{2+} (Figures S2E and S2F), which decreased the Cad^{TS} FRET signal in the front of the cluster, as expected for increased force (Figure S2G). We conclude that the reproducible and significant difference in FRET reports a difference in tension on E-cadherin, which reflects differences in the strength of adhesive bonds and/or actomyosin contractility between the front and the back.

Morphodynamic profiling, a quantitative approach to analysis of migration phenotypes

Since we found E-cadherin to be required for proper direction sensing, we investigated the relationship between E-cadherin and the two chemoattractant receptors known to guide border cells: the platelet-derived growth factor receptor homolog (PVR) and the epidermal growth factor receptor homolog (EGFR) (Duchek et al., 2001; McDonald et al., 2006). Concurrent inhibition of both receptors results in a severe migration defect (Duchek et al., 2001; Prasad and Montell, 2007). We developed image analysis and statistical methods to quantify local protrusion and retraction behavior of migrating border cell clusters in order to compare migration phenotypes in detail. This morphodynamic profiling approach entails identifying the outline of the border cell cluster in each frame of a time-lapse movie followed by mapping the outline in one frame onto the outline in the consecutive frame, thus defining local displacements along the cluster boundary (Figure 4A). We divided the outline into 30 segments and determined the boundary motion as the per-segment average of the local displacement vectors. These segmental values, positive for protrusion, negative for retraction, were then displayed time-point by time-point along the cluster boundary as columns of a matrix referred to as a “morphodynamic activity map” (Figure 4B; Movie S8). Importantly, morphodynamic activity maps are independent of the cluster shape, making it possible to pool maps of multiple experiments of the same genotype.

We first probed the morphodynamic behaviors of clusters in which guidance signaling was disrupted. We expressed dominant-negative constructs for either EGFR (EGFR^{DN}), PVR

(PVR^{DN}), or both receptors (RTK^{DN}), and compared them to the behaviors of WT clusters (see Supplemental Table 2 for full documentation of all genotypes analyzed). The number of movies per condition was determined such that the experimental variation in morphodynamic activity within a genotype was less than the variation between genotypes, allowing a stringent comparison of the effects of the various constructs on migration behavior. Qualitatively, the morphodynamic activity of WT (Figure 4C) and RTK^{DN} (Figure 4D) clusters differed in two obvious properties: First, a distinct front-back polarity was evident in WT clusters, which showed spatially segregated protrusion and retraction with high protrusion velocities predominating at the front and high retraction velocities at the back (Figures 4B-4C). This spatial segregation was lost in clusters lacking guidance receptor activities (Figure 4D). Second, RTK^{DN} clusters displayed overall slower protrusion and retraction velocities. This suggests that reduced guidance signaling not only impedes the polarization of protrusion and retraction events but also dampens the overall level of activation of the mechanical pathways that drive protrusion and retraction events.

To quantify these observations we generated distributions of protrusion velocities in the front and retraction velocities in the rear of the clusters (Figures 4F and 4G) and extracted 24 additional properties from the activity maps to describe the cluster behavior in a morphodynamic profile with 26 features (Supplemental Table 3). For each pairwise combination of genotypes we counted how many features differed at p-value levels of 0.05 and 0.001 (Figures 4H and 4I). Consistent with previous studies (Duchek et al., 2001) we found that expression of EGFR^{DN} alone did not significantly alter morphodynamics compared to WT, but expression of EGFR^{DN} and PVR^{DN} together (RTK^{DN}) did change morphodynamics compared to PVR^{DN} alone. This suggests some overlap in function between the two guidance receptors with respect to front-back polarization of protrusion and retraction events. However PVR is the main receptor activating protrusion and retraction because these velocities are statistically indistinguishable between PVR^{DN} and RTK^{DN}.

Next we compared the morphodynamic profiles of RTK^{DN} clusters to those expressing a dominant-negative construct of Rac1, the main Rho GTPase that is required for border cell migration downstream of RTK signaling (Murphy and Montell, 1996; Geisbrecht and Montell, 2004, Wang et al, 2010; Duchek et al., 2001; Fernandez-Espartero et al., 2013). Confirming the qualitative difference between the morphodynamic activity maps evident from visual inspection (compare Figures 4D and 4E), the two genotypes were different in nearly all features of the profiles, irrespective of whether we tested them at a p-value of 0.05 or 0.001. This suggested that in addition to PVR and EGFR another signal activates Rac1 during directed border cell migration. Comparison of Rac^{DN} with Rac^{DN} + RTK^{DN} corroborated this conclusion, as these two genotypes also differed significantly, albeit less strongly than RTK^{DN} and Rac^{DN}: at a p-value level of 0.001 only 5 out of 26 morphodynamic features were different (Figure 4I).

Tie is a third potential guidance receptor (Wang et al., 2006), and the addition of a dominant negative of Tie shifted the RTK^{DN} profile towards the Rac^{DN} profile in several features (Figures 4H and 4I), including the protrusion and retraction velocities (Figures 4F and 4G). However, there were still significant differences between these two conditions suggesting that other pathways must be involved in the activation Rac.

Morphodynamic profiling reveals that E-cadherin and the chemotactic receptors function in the same process

In view of the border cell guidance defects induced by E-cadherin RNAi, we compared the morphodynamic activities of EcadRNAi-expressing border cells to those expressing RTK^{DN} or EcadRNAi and RTK^{DN}. The profiles of these genotypes appeared strikingly similar (Figure 4D, Figures S4A-S4B), and they were statistically indistinguishable (0 out of 26 features were different between RTK^{DN} and EcadRNAi at both $p < 0.05$ and $p < 0.001$). This applies to the protrusion and retraction velocities at the front and rear of the cluster (Figures 5A-5D), but also to features that quantify the level of front-back polarity such as the percentage of protruding segments at the cluster front or back and the percentage of retracting segments at the cluster front or back. Features that relied on the fraction of protruding versus retracting versus quiescent segments required a threshold that distinguishes moving from quiescent segments. Thus, if the velocity distributions of the genotypes were differentially skewed these features could be similar for one threshold, but different for another. To test this we performed a velocity threshold sweep between 2 and 4 pixels / frame (0.32-0.64 $\mu\text{m}/\text{min}$) and found that the similarity between the genotypes is conserved for the entire range of thresholds (Figures 5E-5H; Figures S4C-S4F for the comparison of EcadRNAi vs. RTK^{DN}+EcadRNAi, and Figures S4G-S4J for the comparison of RTK^{DN} vs. RTK^{DN}+EcadRNAi). We chose the lower threshold value at 2 pixels / frame considering that instantaneous protrusion and retraction velocities below this value would be increasingly contaminated by noise and thus could bias the comparison. Based on the robust similarity between the morphodynamic effects of reducing E-cadherin expression or guidance receptor activity, we conclude that E-cadherin functions in the same process as EGFR and PVR to guide the migrating border cells to the oocyte.

Chemotactic guidance cues promote tension on E-cadherin

To further examine the relationship between the chemotactic guidance cues and E-cadherin, we analyzed the distribution of tension on E-cadherin in border cell clusters expressing PVR^{DN} and EGFR^{DN} (Figures 6A and 6B). In such clusters the front to back FRET ratios of both the Cad^{TS} and the control were close to 1 (Figure 6E), suggesting that the force asymmetry in WT depends on guidance receptor activity and that tension on E-cadherin is generated downstream of chemotactic receptors.

Since Rac also functions downstream of the RTKs (Duchek et al., 2001; Wang et al., 2010; Fernandez-Espartero et al., 2013), we tested whether the RTKs signal to E-cadherin through Rac. Expressing a DN form of Rac (Rac^{DN}) indeed caused the front/back Cad^{TS} FRET ratio to rise close to 1, whereas there was no significant change in the load-insensitive control sensor (Figures 6C, 6D and 6F). The front/back ratio could change either due to a change at the front, the back, or both. We found that Rac^{DN} increased the FRET index primarily at the front of the cluster (Figure 6G) but not significantly at the back (Figure S2I), indicating that Rac functions at the front of the migrating cluster to increase tension on E-cadherin-mediated adhesions, consistent with its normally higher activity at the front (Wang et al., 2010).

E-cadherin reinforces Rac signaling at the cluster front via positive feedback

Polarization and directional persistence in migrating cells are thought to require feedback amplification mechanisms (Charest and Firtel, 2006; Iglesias and Devreotes, 2012). To test if E-cadherin mediates directional persistence in border cell migration by positive feedback onto Rac activity, we used a Rac FRET probe to monitor the Rac activity pattern. Compared to the WT Rac-FRET pattern, where the highest FRET is reproducibly at the front of the cluster (Figures 6H and 6N), knocking down E-cadherin in the border cells randomized the distribution of Rac-FRET (Figures 6I-6K and 6N) consistent with the lack of directional persistence (Figures 1I and 1K). The total Rac-FRET level was slightly decreased although this did not rise to statistical significance (Figure 6O). Together with the finding that the establishment of a tension gradient on E-cadherin depends on Rac-mediated signaling from chemotactic receptors this result puts E-cadherin in a feedback loop that amplifies the output of RTK activity and leads to higher Rac activity at the front, thus promoting polarization of the border cell cluster and directionally persistent migration.

Although PVF1 is a key guidance signal for the border cells, we could not detect a significant gradient of PVF1 along the migration path (Figure 6P), and previous studies have failed to detect a difference in the concentration of activated receptor at the front compared to the back of the cluster except when the receptor is over-expressed (Janssens et al., 2010). This probably means that the concentration difference is normally small and artificially amplified by over-expression of the receptor. Unexpectedly, we detected a statistically significant gradient in E-cadherin concentration along the migration path (Figure 6Q). Although, as mentioned above, there is no measurable difference in E-cadherin concentration between the front and the back of border cell clusters, this is likely due to the shallowness of the E-cadherin concentration gradient; the difference over 20-30 μm is simply not large enough to measure. Taken together these observations suggest that small differences in E-cadherin and PVF1/PVR signaling are amplified by positive feedback into a larger difference in Rac signaling across the cluster, which establishes strong and stable forward protrusion required for directionally persistent migration.

Directed, collective migration requires not only stable front protrusion but also inhibition of protrusion by back and side cells of the cluster. We previously showed that photo-activation of Rac in one cell is sufficient to set the direction of migration for the whole group (Wang et al, 2010). Moreover photo-inhibition of Rac in the lead cell causes the other cells to lose their sense of direction, retract the forward-directed protrusion, and extend protrusions in other directions (Figure 7A and Figures S5A-S5C). One mechanism by which the front cell could inhibit protrusion of the neighboring cells could be through mechanical coupling of the cells via cell-cell adhesions. Therefore we examined the effect of photo-inhibiting Rac in the lead cell following k.d. of adherens junction components. RNAi of either E-cadherin, β -catenin or α -catenin prevented cell-to-cell communication of directional information such that side and rear cells failed to respond when Rac was inhibited in the front cell (Figure 7A, Figures S5G-S5O). As a negative control we examined the effect of N-cadherin RNAi. N-cadherin expression is undetectable in migrating border cells and as expected N-cadherin RNAi did not prevent extension of protrusions by other cells (Figure 7A, Figures S5D-S5F). To rule out the possible caveat that E-cadherin, β -catenin and α -catenin were simply

required for the other cells to make protrusions, we repeated PA-Rac^{DN} experiments using FLP OUT clones to express PA-Rac^{DN} with or without the RNAi lines in one single cell of the cluster. Photo-inhibiting Rac in this one cell caused other cells to send out extra protrusions (Figure 7B), while knocking down the components of adherens junction in this one cell prevented the effect (Figure 7B, Figures S5P-S5U). Therefore border cell-border cell adhesion mediated by E-cadherin is required for communication of direction between the cells of the cluster and thus for collective direction sensing.

Discussion

To characterize the molecular mechanisms of collective migration of cells in between other cells in a living tissue, we developed two new approaches: morphodynamic profiling and an *in vivo* optical sensor of mechanical tension on E-cadherin. We used them in combination with photo-inhibitable Rac, cell-type-specific RNAi and live imaging to reveal that E-cadherin-mediated adhesion serves multiple critical functions, each in a distinct subcellular location (Figure 7Ci). First and most intriguingly, border cell-nurse cell adhesion functions in a feedback loop with Rac downstream of guidance RTK signaling to stabilize forward-directed protrusion and generate a stable front (Figures 7Cii and 7Ciii). Second, border cell-border cell adhesion transmits directional information within the group so that the lead cell communicates direction to side and back cells (Figure 7Civ). Finally, border cell-polar cell adhesion holds the cluster together ensuring collective behavior, and provides a polarity to each cell that biases protrusion outward toward the border cell-nurse cell interface (Figure 7Cv). This combination of effects confers a polarity for protrusion onto each individual motile cell and then endows the entire cluster with an overall front/back polarity that supports directionally persistent collective migration.

Positive feedback amplification generates a stable front of the migrating cluster

A longstanding problem in chemotaxis is how individual cells can create a robust difference in protrusion/retraction behavior between the front and back, even when there is as little as a 1% difference in ligand concentration and receptor activation (e.g., Meinhardt, 1999). Local positive feedback is thought to amplify the protrusive response at the front where it dominates over a weaker global inhibition of protrusion. The underlying molecular mechanisms are under intense investigation (Iglesias and Devreotes, 2012; Houk et al., 2012). Our data show that positive feedback between Rac and E-cadherin at the leading edge is essential for stable front protrusion in migrating border cells (Figure 7Cii).

Detecting tension asymmetry in vivo

Consistent with a role for E-cadherin in generating front/back polarity, we measured a difference in the tension across E-cadherin molecules at the front compared to the back of the cell cluster. Elevated tension at the front is informative because in principle cells could detach at the rear either by “ripping” up the adhesions or by reducing the strength of the adhesion. The high tension on E-cadherin at the front suggests that cells actively disassemble adhesions at the back. High tension also suggests that either the strength of the E-cadherin/E-cadherin bonds is stronger and/or that force generated by the cytoskeleton is stronger at the front, or both. The possibility that E-cadherin/E-cadherin bonds might be

stronger at the front is supported by the observation *in vitro* E-cadherin can form catch bonds, which are E-cadherin/E-cadherin bonds that strengthen under force (Rakshit et al., 2012). As for force generated by the cytoskeleton, there are two primary mechanisms of force generation in directed protrusion, both of which likely contribute to tension on E-cadherin (Figure 7D): actin filament assembly propels the cell edge outward, and actomyosin contraction pulls it inward. Actin filament assembly should generate tension on E-cadherin by propelling the leading edge forward, which generates membrane tension due to stretching of the plasma membrane and therefore an equal pushing force in the direction opposite to the protrusion (Figure 7D). In addition, actin polymerization likely generates retrograde flow that is resisted by E-cadherin-mediated adhesion between border cells and nurse cells. This mechanism is analogous to that reported for integrin-mediated cell-matrix adhesions at the leading edge of epithelial cells, where forces across adhesions are spatially and temporally co-modulated with filament assembly (Ji et al., 2008). This mechanism provides an attractive explanation for the positive feedback between E-cadherin and Rac signaling.

The precise biochemical mechanism by which mechanically loaded E-cadherin stimulates Rac activity has yet to be determined, however plausible mechanisms have been described. For example, when VE-cadherin on one endothelial cell engages VE-cadherin on another cell, Rac exchange factors are recruited, which activate Rac locally (Birukova et al., 2012). Since Rac promotes actin filament assembly and protrusion, which stabilizes E-cadherin/E-cadherin adhesions, this could provide a simple and direct feedback. Thus, we propose that E-cadherin operates as the mechanotransducer in a mechanochemical feedback between actin network propulsion and Rac signaling that amplifies the activation of Rac signaling by guidance cues in order to establish robust front protrusion and directionally persistent motility.

E-cadherin-mediated adhesion between migratory border cells polarizes the cluster

In collective cell migrations, directional movement requires that protrusion be prevented in the side and back cells. We previously showed that photo-activation of Rac in any cell of the migrating cluster can cause the other cells to retract protrusions and follow the cell with the highest Rac activity. In addition, photo-inhibition of Rac in one cell of the cluster causes the other cells to lose their sense of direction and protrude outward (Wang et al., 2010). Here we report that E-cadherin-mediated adhesion between border cells mediates this cell-cell communication. Moesin, which links cortical F-actin to the plasma membrane, and Rab11 are also required for this cell-cell communication during collective guidance (Ramel et al, 2013). Together these findings suggest that when the lead cell protrudes and pulls on the other cells of the cluster, E-cadherin adhesions and the cortical F-actin cytoskeleton transduce mechanical force to side and rear cells inhibiting them from protruding (Figure 7Civ).

Each individual border cell is also polarized such that it is more likely to protrude away from polar cells, where the E-cadherin concentration is highest and toward nurse cells where it is lowest (Figure 7Cv). Concentrated E-cadherin at the polar cell/border cell boundary may serve the function of contact inhibition of protrusion, similar to the function of

cadherins in other examples of collective migration (Carmona-Fontaine et al., 2008; Weber et al., 2012).

Multiple positive roles for E-cadherin could contribute to diversify migrations *in vivo*

Although *in vitro* studies of cell migration have focused extensively on single cells migrating on ECM, it is clear that *in vivo*, migration modes are extremely diverse. Additional examples of cells requiring cadherin-mediated adhesion to hold them together include collectively migrating neural crest cells (Theveneau and Mayor, 2012), MDCK cells (Shih and Yamada, 2012), germ cell progenitors in zebrafish (Arboleda-Estudillo et al., 2010), and cell sheets (Ng et al., 2012; Vitorino and Meyer, 2008). Examples of cells requiring cadherin for adhesion to the cells they migrate on or between include primordial germ cells in zebrafish (Kardash et al., 2010) and *Drosophila* (Kunwar et al., 2008), and mouse retinal endothelial cells (Gariano and Gardner, 2005).

The distinct roles for E-cadherin we discovered in the context of border cell migration need not always occur together in the same migration event. Single cells migrating over the surfaces of other cells might use the amplification feedback loop between Rac and E-cadherin, without a requirement for adhesion with other migrating cells. Collectively migrating cells moving on basement membranes or through interstitial matrices might employ cell-cell adhesion for coordinating their movement while using integrin in a feedback loop with Rac to stabilize front protrusions. Thus, we propose that the various mechanisms described here could function as modules that can be combined in various ways with or without cell-matrix adhesion and chemotactic responses to diversify morphogenetic cell movements *in vivo*.

Experimental Procedures

Drosophila strains and genetics

Gal4 drivers include *slbo*Gal4 (Rorth, 1998), *upd*Gal4 (a gift from Douglas Harrison), *triple*Gal4 (*MTD-Gal4*, Bloomington #31777), *nos*Gal4 (Van Doren et al., 1998). Three UAS-EcadRNAi lines were used: GD27082, KK103962 [Vienna *Drosophila* RNAi Center (VDRC), for border cell-specific knockdown], and #32904 (Bloomington *Drosophila* Stock Center, border cell and nurse cell-specific knock down). UAS-PVR^{DN}, UAS-EGFR^{DN}, UAS-Rac^{DN}, UAS-Rac-FRET and UAS-PA-Rac^{T17N} were described previously (Wang et al., 2010). UAS-NcadRNAi, UAS-Arm RNAi, and UAS- α -cat RNAi flies were obtained from VDRC. All the lines and crosses were kept at 25°C unless otherwise indicated. Newly eclosed flies were collected and kept on food without yeast for 2-3 days. Before dissection, flies were fattened at 25°C with dry yeast overnight. RNAi lines were fattened at 29°C.

Transgenic flies

For Cad^{TS} flies, tension sensor module was inserted between the transmembrane domain and β -catenin binding site of full length *Drosophila* E-cadherin. For control flies, tension sensor module was inserted before the E-cadherin stop codon. Both Cad^{TS} and control constructs were cloned downstream of a ubiquitin promoter. LifeactGFP and LifeactRFP were amplified from constructs described in (Riedl et al., 2008), and cloned downstream of a

slbo or UAS promoter, respectively. Primers and molecular cloning procedures are described in Supplemental Information.

Live-imaging and data processing

Time-lapse imaging was carried out as previously described (Prasad et al., 2007). Rolling ball background-subtraction was done in the GFP channel. Migration tracks were drawn using Imaris software. Directional persistence was calculated by dividing the x-axis migration path length by total migration track length. Directionality index was calculated as: (# of front-directed protrusion)/(# of total protrusion) in the entire movie. Migration speed was calculated as described before (Wang et al., 2010).

FRET images were collected from living egg chambers using a Zeiss LSM 710 microscope. A 458nm laser was used for excitation, and mTFP/Venus images were acquired simultaneously using channel 1 (463-501nm) and channel 2 (519-566nm) under 40x/1.1W LD C-Apo lens. Spectral bleed-through analysis and FRET efficiency calculations are detailed in supplemental information. FRET image processing was carried out in NIH ImageJ software as previously described (Wang et al., 2010) and detailed in supplemental Information.

Immunohistochemistry

After dissection, *Drosophila* egg chambers were fixed in 4% paraformaldehyde on ice for 25min. Immunostaining was carried out as previously described (McDonald and Montell, 2005) and detailed in supplemental information. Quantifying E-cadherin and Pvf1 expression along the migration path: migration path was traced using the Freehand Line Tool in ImageJ. Then, the Plot Profile function was used to obtain the mean fluorescence intensity along the migration path. Absolute migration path lengths, in microns, were normalized to % path length, i.e. 1% being the farthest from the oocyte and 100% being closest to the oocyte, to normalize for egg chamber size. These normalized values were then averaged and plotted using the scatter plot function in Microsoft Excel.

Morphodynamic Profiling

Effects of perturbation of guidance receptors, E-cadherin and Rac signaling by RNAi or expression of dominant negative constructs were assessed by multi-parametric analysis of the border cell cluster protrusion and retraction behavior in morphodynamic profiles. These profiles consist of 26 features (Supplemental Table S3), which capture the speed, persistence, and polarity of protrusion and retraction. Profiles of different genotypes were compared feature-by-feature using the randomization test (function `rndtest()` in Matlab), which accounts for the non-normality of the feature distribution. Detailed steps of cluster tracking and derivation of morphodynamic profiles from the cluster boundary motion are described in Supplemental Information.

Photomanipulation of PA-Rac

Photoactivation, time-lapse-imaging, and 3D morphological reconstruction were carried out using a Zeiss 510-Meta confocal microscope using a 63X, 1.4 numerical aperture lens with

2X zoom. 3D reconstructions were rendered using Imaris software. Detailed steps of photo manipulation and identification of protrusions are described in Supplemental Information.

Supplementary Material

Refer to Web version on PubMed Central for supplementary material.

Acknowledgments

We thank the Montell lab for helpful discussions and Craig Montell for insightful comments on the manuscript. We thank the Erika Matunis laboratory and Bloomington Stock Center for generous sharing of fly stocks. This work was supported by GM73164 and GM46425 to DJM, GM64346 (Cell Migration Consortium) to DJM and GD, and GM71868 to GD.

References

- Arboleda-Estudillo Y, Krieg M, Stuhmer J, Licata NA, Muller DJ, Heisenberg CP. Movement directionality in collective migration of germ layer progenitors. *Curr Biol*. 2010; 20:161–169. [PubMed: 20079641]
- Birukova AA, Tian Y, Dubrovskiy O, Zebda N, Sarich N, Tian X, Wang Y, Birukov KG. VE-cadherin trans-interactions modulate Rac activation and enhancement of lung endothelial barrier by iloprost. *Journal of cellular physiology*. 2012; 227:3405–3416. [PubMed: 22213015]
- Borghi N, Sorokina M, Shcherbakova OG, Weis WI, Pruitt BL, Nelson WJ, Dunn AR. E-cadherin is under constitutive actomyosin-generated tension that is increased at cell-cell contacts upon externally applied stretch (vol 109, 12568, 2012). *P Natl Acad Sci USA*. 2012; 109:19034–19034.
- Carmona-Fontaine C, Matthews HK, Kuriyama S, Moreno M, Dunn GA, Parsons M, Stern CD, Mayor R. Contact inhibition of locomotion in vivo controls neural crest directional migration. *Nature*. 2008; 456:957–961. [PubMed: 19078960]
- Charest PG, Firtel RA. Feedback signaling controls leading-edge formation during chemotaxis. *Curr Opin Genet Dev*. 2006; 16:339–347. [PubMed: 16806895]
- Conway DE, Breckenridge MT, Hinde E, Gratton E, Chen CS, Schwartz MA. Fluid Shear Stress on Endothelial Cells Modulates Mechanical Tension across VE-Cadherin and PECAM-1. *Current Biology*. 2013; 23:1024–1030. [PubMed: 23684974]
- Duchek P, Rorth P. Guidance of cell migration by EGF receptor signaling during *Drosophila* oogenesis. *Science*. 2001; 291:131–133. [PubMed: 11141565]
- Duchek P, Somogyi K, Jekely G, Beccari S, Rorth P. Guidance of cell migration by the *Drosophila* PDGF/VEGF receptor. *Cell*. 2001; 107:17–26. [PubMed: 11595182]
- Fernandez-Espartero CH, Ramel D, Farago M, Malartre M, Luque CM, Limanovich S, Katzav S, Emery G, Martin-Bermudo MD. GTP exchange factor Vav regulates guided cell migration by coupling guidance receptor signalling to local Rac activation. *J Cell Sci*. 2013; 126:2285–2293. [PubMed: 23525006]
- Friedl P, Gilmour D. Collective cell migration in morphogenesis, regeneration and cancer. *Nat Rev Mol Cell Biol*. 2009; 10:445–457. [PubMed: 19546857]
- Fulga TA, Rorth P. Invasive cell migration is initiated by guided growth of long cellular extensions. *Nat Cell Biol*. 2002; 4:715–719. [PubMed: 12198500]
- Gariano RF, Gardner TW. Retinal angiogenesis in development and disease. *Nature*. 2005; 438:960–966. [PubMed: 16355161]
- Geisbrecht ER, Montell DJ. A role for *Drosophila* IAP1-mediated caspase inhibition in Rac-dependent cell migration. *Cell*. 2004; 118:111–125. [PubMed: 15242648]
- Grashoff C, Hoffman BD, Brenner MD, Zhou RB, Parsons M, Yang MT, McLean MA, Sligar SG, Chen CS, Ha T, et al. Measuring mechanical tension across vinculin reveals regulation of focal adhesion dynamics. *Nature*. 2010; 466:263–U143. [PubMed: 20613844]

- He L, Wang XB, Tang HL, Montell DJ. Tissue elongation requires oscillating contractions of a basal actomyosin network. *Nature Cell Biology*. 2010; 12:1133-U1140.
- Houk AR, Jilkine A, Mejean CO, Boltyanskiy R, Dufresne ER, Angenent SB, Altschuler SJ, Wu LF, Weiner OD. Membrane Tension Maintains Cell Polarity by Confining Signals to the Leading Edge during Neutrophil Migration. *Cell*. 2012; 148:175–188. [PubMed: 22265410]
- Iglesias PA, Devreotes PN. Biased excitable networks: how cells direct motion in response to gradients. *Curr Opin Cell Biol*. 2012; 24:245–253. [PubMed: 22154943]
- Janssens K, Sung HH, Rorth P. Direct detection of guidance receptor activity during border cell migration. *P Natl Acad Sci USA*. 2010; 107:7323–7328.
- Ji L, Lim J, Danuser G. Fluctuations of intracellular forces during cell protrusion. *Nature Cell Biology*. 2008; 10:1393-U1338.
- Kalluri R, Weinberg RA. The basics of epithelial-mesenchymal transition. *J Clin Invest*. 2009; 119:1420–1428. [PubMed: 19487818]
- Kardash E, Reichman-Fried M, Maitre JL, Boldajipour B, Papusheva E, Messerschmidt EM, Heisenberg CP, Raz E. A role for Rho GTPases and cell-cell adhesion in single-cell motility in vivo. *Nat Cell Biol*. 2010; 12:47–53. sup pp 41-11. [PubMed: 20010816]
- Kunwar PS, Sano H, Renault AD, Barbosa V, Fuse N, Lehmann R. Tre1 GPCR initiates germ cell transepithelial migration by regulating *Drosophila melanogaster* E-cadherin. *J Cell Biol*. 2008; 183:157–168. [PubMed: 18824569]
- McDonald JA, Montell DJ. Analysis of cell migration using *Drosophila* as a model system. *Methods Mol Biol*. 2005; 294:175–202. [PubMed: 15576913]
- McDonald JA, Pinheiro EM, Kadlec L, Schupbach T, Montell DJ. Multiple EGFR ligands participate in guiding migrating border cells. *Dev Biol*. 2006; 296:94–103. [PubMed: 16712835]
- Meinhardt H. Orientation of chemotactic cells and growth cones: models and mechanisms. *J Cell Sci*. 1999; 112:2867–2874. [PubMed: 10444381]
- Montell DJ, Rorth P, Spradling AC. Slow Border Cells, a Locus Required for a Developmentally Regulated Cell-Migration during Oogenesis, Encodes *Drosophila* C/Ebp. *Cell*. 1992; 71:51–62. [PubMed: 1394432]
- Montell DJ, Yoon WH, Starz-Gaiano M. Group choreography: mechanisms orchestrating the collective movement of border cells. *Nat Rev Mol Cell Bio*. 2012; 13:631–645. [PubMed: 23000794]
- Murphy AM, Montell DJ. Cell type-specific roles for Cdc42, Rac, and RhoL in *Drosophila* oogenesis. *J Cell Biol*. 1996; 133:617–630. [PubMed: 8636236]
- Ng MR, Besser A, Danuser G, Brugge JS. Substrate stiffness regulates cadherin-dependent collective migration through myosin-II contractility. *Journal of Cell Biology*. 2012; 199:545–563. [PubMed: 23091067]
- Niessen CM, Leckband D, Yap AS. Tissue organization by cadherin adhesion molecules: dynamic molecular and cellular mechanisms of morphogenetic regulation. *Physiological reviews*. 2011; 91:691–731. [PubMed: 21527735]
- Niewiadomska P, Godt D, Tepass U. DE-cadherin is required for intercellular motility during *Drosophila* oogenesis. *Journal of Cell Biology*. 1999; 144:533–547. [PubMed: 9971747]
- Prasad M, Jang AC, Starz-Gaiano M, Melani M, Montell DJ. A protocol for culturing *Drosophila melanogaster* stage 9 egg chambers for live imaging. *Nat Protoc*. 2007; 2:2467–2473. [PubMed: 17947988]
- Prasad M, Montell DJ. Cellular and molecular mechanisms of border cell migration analyzed using time-lapse live-cell imaging. *Dev Cell*. 2007; 12:997–1005. [PubMed: 17543870]
- Rakshit S, Zhang Y, Manibog K, Shafraz O, Sivasankar S. Ideal, catch, and slip bonds in cadherin adhesion. *Proc Natl Acad Sci U S A*. 2012; 109:18815–18820. [PubMed: 23112161]
- Ramel D, Wang XB, Laflamme C, Montell DJ, Emery G. Rab11 regulates cell-cell communication during collective cell movements. *Nature Cell Biology*. 2013; 15:317–324.
- Riedl J, Crevenna AH, Kessenbrock K, Yu JH, Neukirchen D, Bista M, Bradke F, Jenne D, Holak TA, Werb Z, et al. Lifeact: a versatile marker to visualize F-actin. *Nat Methods*. 2008; 5:605–607. [PubMed: 18536722]

- Rorth P. Gal4 in the *Drosophila* female germline. *Mech Dev.* 1998; 78:113–118. [PubMed: 9858703]
- Shih W, Yamada S. N-cadherin-mediated cell-cell adhesion promotes cell migration in a three-dimensional matrix. *J Cell Sci.* 2012; 125:3661–3670. [PubMed: 22467866]
- Theveneau E, Mayor R. Cadherins in collective cell migration of mesenchymal cells. *Curr Opin Cell Biol.* 2012; 24:677–684. [PubMed: 22944726]
- Van Doren M, Williamson AL, Lehmann R. Regulation of zygotic gene expression in *Drosophila* primordial germ cells. *Current Biology.* 1998; 8:243–246. [PubMed: 9501989]
- Vitorino P, Meyer T. Modular control of endothelial sheet migration. *Gene Dev.* 2008; 22:3268–3281. [PubMed: 19056882]
- Wang X, He L, Wu YI, Hahn KM, Montell DJ. Light-mediated activation reveals a key role for Rac in collective guidance of cell movement in vivo. *Nat Cell Biol.* 2010; 12:591–597. [PubMed: 20473296]
- Wang XJ, Bo JY, Bridges T, Dugan KD, Pan TC, Chodosh LA, Montell DJ. Analysis of cell migration using whole-genome expression profiling of migratory cells in the *Drosophila* ovary. *Developmental Cell.* 2006; 10:483–495. [PubMed: 16580993]
- Weber GF, Bjerke MA, DeSimone DW. A Mechanoresponsive Cadherin-Keratin Complex Directs Polarized Protrusive Behavior and Collective Cell Migration. *Developmental Cell.* 2012; 22:104–115. [PubMed: 22169071]

Highlights

- E-cadherin functions in a feedback loop with Rac to promote stable forward protrusion
- An *in vivo* optical E-cadherin tension sensor reveals asymmetric tension
- Border cell-nurse cell adhesion is required for cluster polarization
- Border cell-border cell adhesion mediates front/back communication

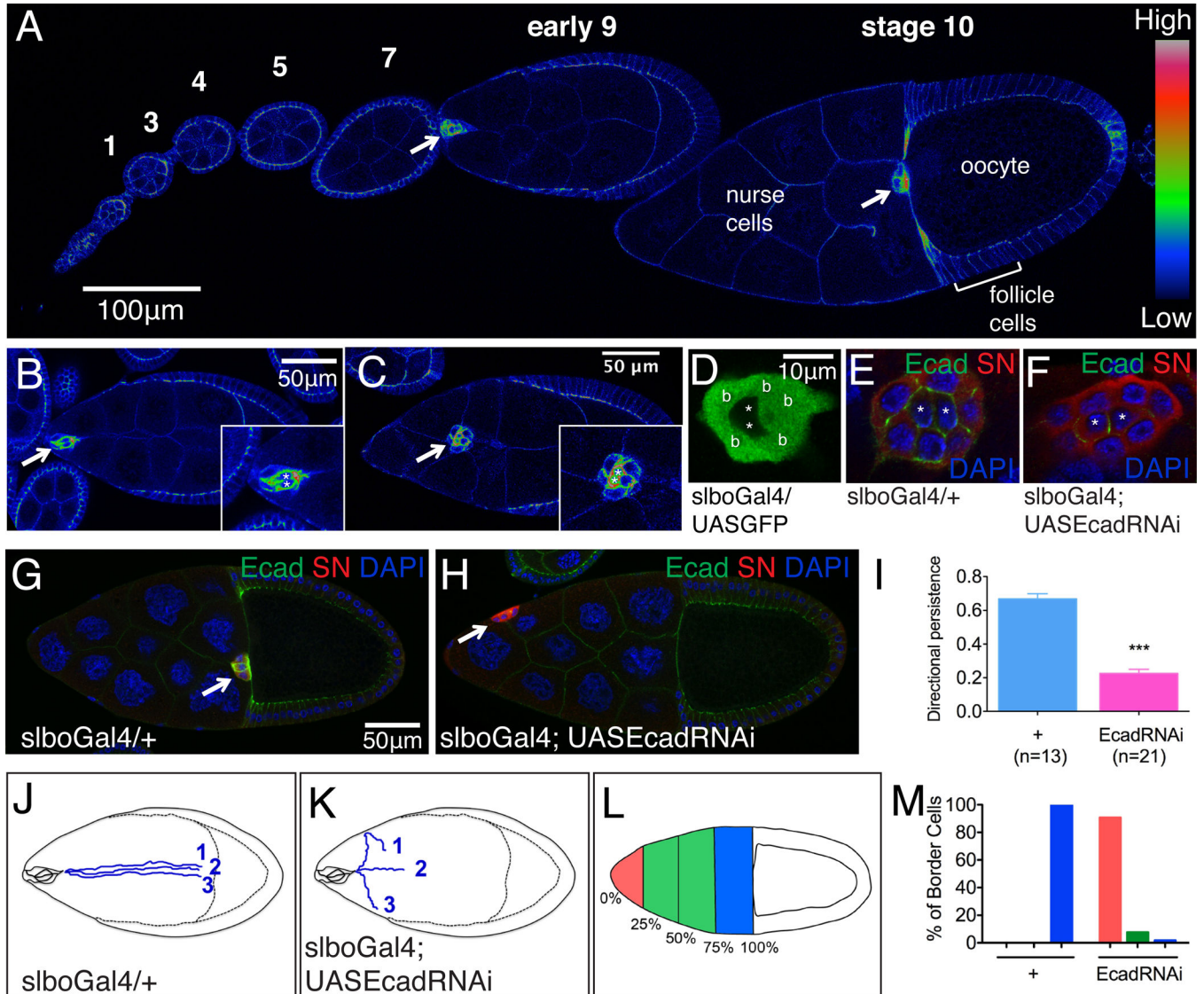


Figure 1. E-cadherin expression and k.d. phenotypes in border cells

(A-C) E-cadherin antibody staining. (A) One ovariole with stages 1-10 of egg chamber development. Early (B) and mid (C) stage 9 egg chambers. Images are pseudo-colored (using Rainbow RGB in Image J) to emphasize spatial differences in E-cadherin concentration. Arrows indicate border cell clusters. Insets show magnified views. Asterisks mark polar cells. (D-F) Specific inhibition of E-cadherin in outer, migratory cells. (D) *slboGal4*-driven expression of GFP in outer migratory cells, not polar cells (*). (E) Normal expression of E-cadherin (Ecad, green) in border cells and polar cells. (F) Inhibition of Ecad expression by *slboGal4* driven RNAi in outer border cells, not polar cells (*). In E and F, nuclei are labeled with DAPI (blue) and cytoplasm with Singed (SN) antibody (red). (G) WT stage 10 egg chamber showing normal migration of border cells (arrow) to the oocyte. (H) Abnormal position of border cells (arrow) following inhibition of Ecad expression by *slboGal4* driven RNAi. (I) Directional persistence values calculated from movies. Genotypes are *slboGal4*; UAS-dsRed, UASmCD8 GFP with or without UAS EcadRNAi.

*** $p < 0.001$. Data are presented as mean \pm SEM. (J-K) Diagrams showing three representative traces of migration paths from movies of WT (J) and Ecad RNAi border cell clusters (K). (L-M) Histogram showing the spatial distribution of border cells in stage 10 egg chambers from *slboGal4* females with or without UASEcadRNAi.

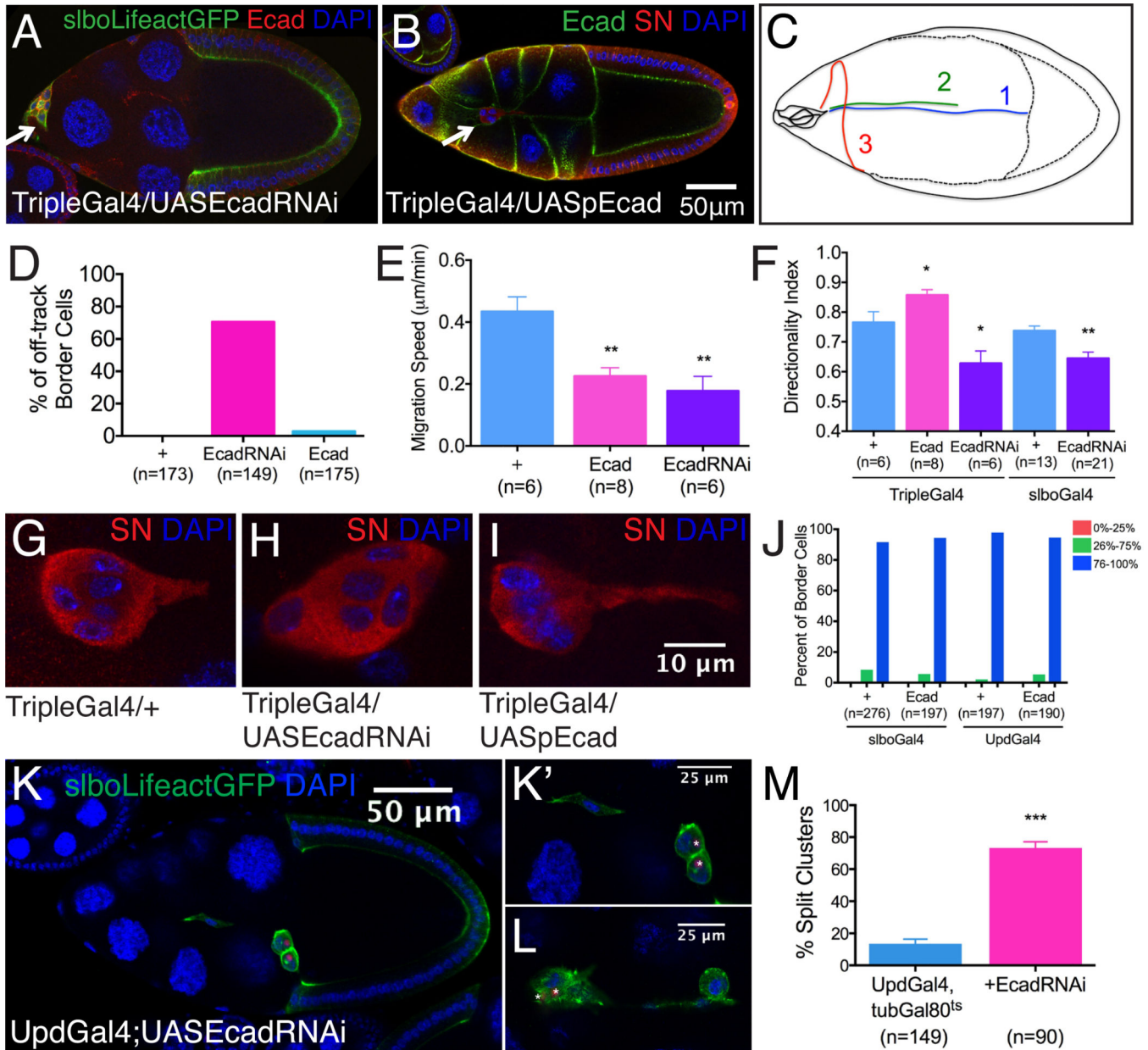


Figure 2. Effects of germline and polar cell E-cadherin RNAi or over-expression on border cell migration

(A-B) Distribution of E-cadherin in stage 10 egg chambers following nurse cell-specific Ecad RNAi (A) or overexpression (B). Border cell cluster positions are marked by arrows.

(C) Diagram showing representative migration paths of 1.WT; 2.TripleGal4, UASpEcad; 3.TripleGal4, EcadRNAi border cells.

(D-F) Quantification of migration phenotypes.

* $p < 0.05$; ** $p < 0.005$. Data are presented as mean \pm SEM. (G-I) Magnified views of border cell clusters of the indicated genotypes showing the effects of inhibition (H) or over-expression (I) of E-cadherin in the germline on border cell protrusion.

(J) Quantification of border cell migration at stage 10 with or without full length E-cadherin overexpression in border cells using *slboGal4* or polar cells using *UpdGal4*.

(K-M) Stage 10 egg chambers

expressing EcadRNAi in polar cells (K) and higher magnification view (K'). (L) A second example. Border cell clusters are marked by slboLifeactGFP. Polar cells express nuclear dsRed. (M) Quantification of split clusters in UpdGal4, tubGal80^{ts} with or without UASEcadRNAi. ***p<0.001. Data are presented as mean ± SEM.

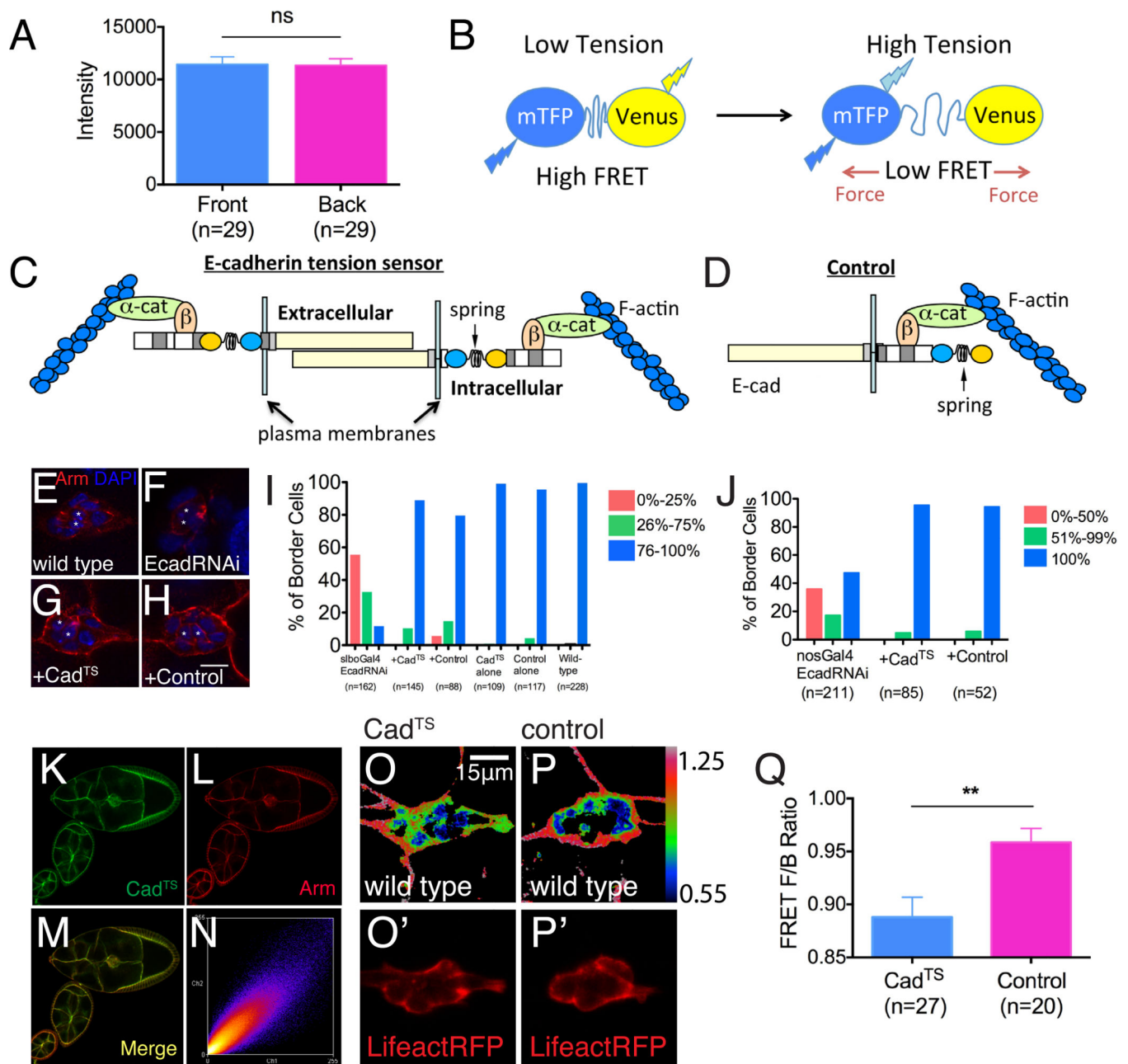


Figure 3. An *in vivo* E-cadherin tension sensor

(A) Quantification of E-cadherin immunofluorescence intensity at the front and back of migrating border cell clusters. Data are presented as mean \pm SEM. (B) Schematic drawing of the tension-sensing (TS) module. Teal fluorescent protein (mTFP) is separated from Venus, a yellow fluorescent protein, by a nano-spring protein domain from spider silk. In the relaxed state, the two fluorophores are close enough to allow FRET. The spider silk domain stretches in response to pico Newton forces, reducing FRET (Grashoff et al., 2010 see text and Experimental Procedures for details). (C) Schematic of the E-cadherin tension sensor (Cad^{TS}), and (D) a corresponding control construct, which should not be tension-sensitive. (E-H) Rescue of Armadillo expression (Arm, which is *Drosophila* β -catenin) in border cells

after EcadRNAi (F) by Cad^{TS} (G) and control (H). Polar cells are marked by asterisks. Scale bar shows 10 μ m. (I-J) Histograms showing Cad^{TS} and control rescuing border cell migration after border cells-specific (I) and nurse cell-specific (J) EcadRNAi. (K-N) Colocalization of Cad^{TS} with Arm. (O-P') FRET images of border cell Cad^{TS} (O) and control (P) pseudo-colored in Rainbow RGB. The outlines of border cells are shown by Lifeact-RFP which is co-expressed in the same experiment (O', P'). (Q) Histogram showing the front to back FRET ratios for Cad^{TS} (blue) and control (pink). Data are presented as mean \pm SEM. **p<0.005. See also Supplemental Figure S2.

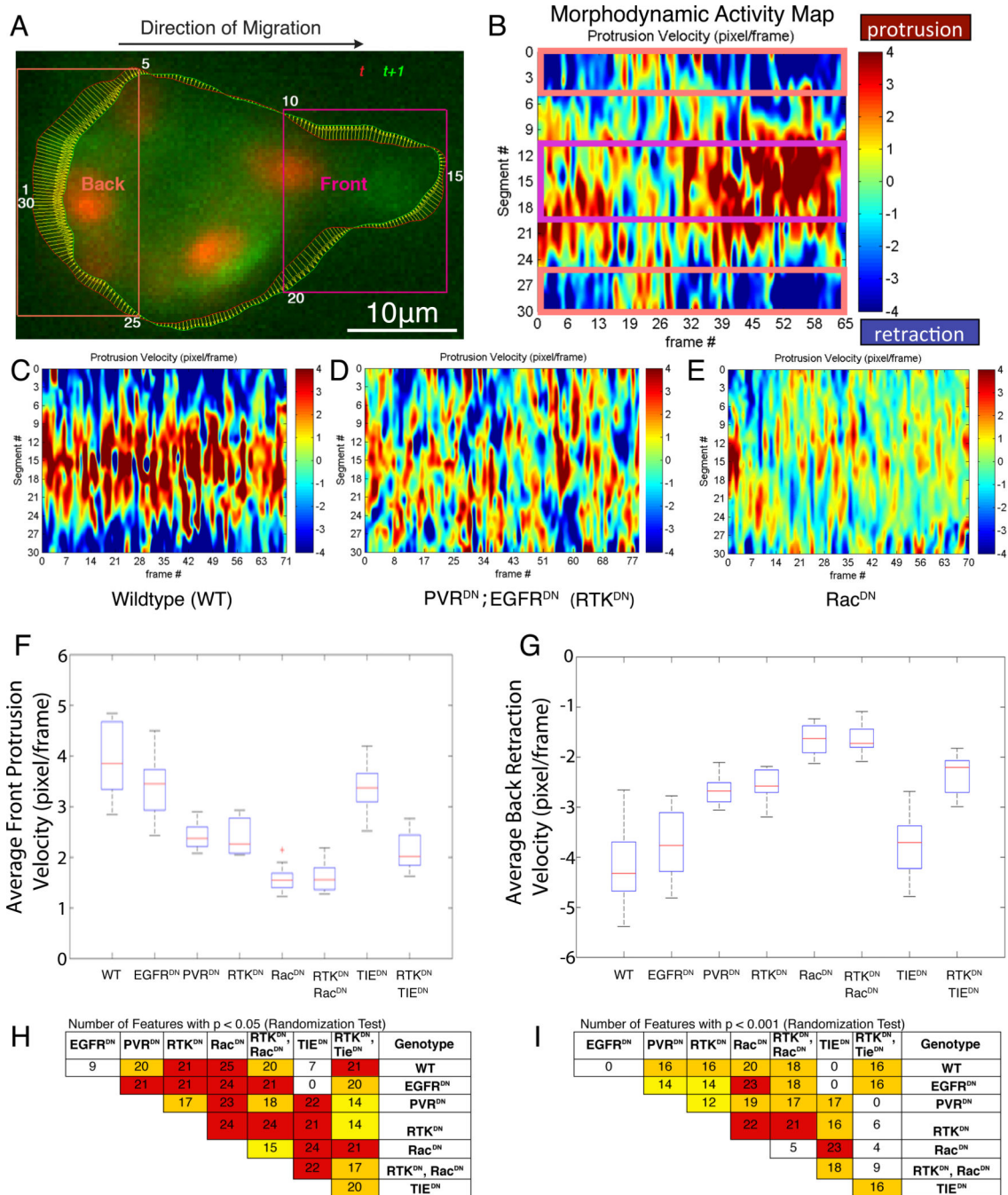


Figure 4. Morphodynamic profiling of border cell migration

(A) Border cell cluster labeled with nuclear dsRed and mCD8GFP. Overlaid are the cluster outlines at t (red) and $t+1$ (green), and local displacement vectors mapping corresponding outline points between the time points. Local displacement vectors were binned and averaged in 30 boundary segments of equal length (enumerated clockwise). Purple boxes highlight the cluster front and back as defined by the boundary segment (front, segments 10-20; back segments 25-30 and 1-5). Scalebar: 10 μ m. (B) Segmental average velocities were mapped time point by time point into the columns of a matrix referred to as

morphodynamic activity map and color coded for visualization (red colors, protrusion; blue colors, retraction). (C-E) Representative morphodynamic activity maps for a WT cluster (C), and for clusters expressing dominant negative constructs of EGFR and PVR guidance receptors (collectively referred to as RTK^{DN}) (D), and of their downstream effector Rac1 (Rac^{DN}) (E). (F, G) Comparison of genotypes related to chemotactic guidance signaling in terms of the average velocity of protruding segments at the front and retracting segments at the back. Box plots (boxes indicate 25%, 50%, and 75% quantiles; whiskers indicate 95% range) show the distributions of the per-cluster averages. Each condition has been measured in at least 8 repeats (see Supplemental Table S2 for documentation of data sets). (H, I) Profiles consisting of 26 features (see Supplemental Table S3) were extracted from morphodynamic activity maps. Tables show for pairwise comparison how many features differed between indicated genotypes using randomization tests of individual features. Tests were run at p-value thresholds $p < 0.05$ (H) and $p < 0.001$ (I). White, < 10 features differ; yellow, 10 – 15 features differ; orange, 16 – 20; red, >20 features differ. See also Supplemental Figure S3.

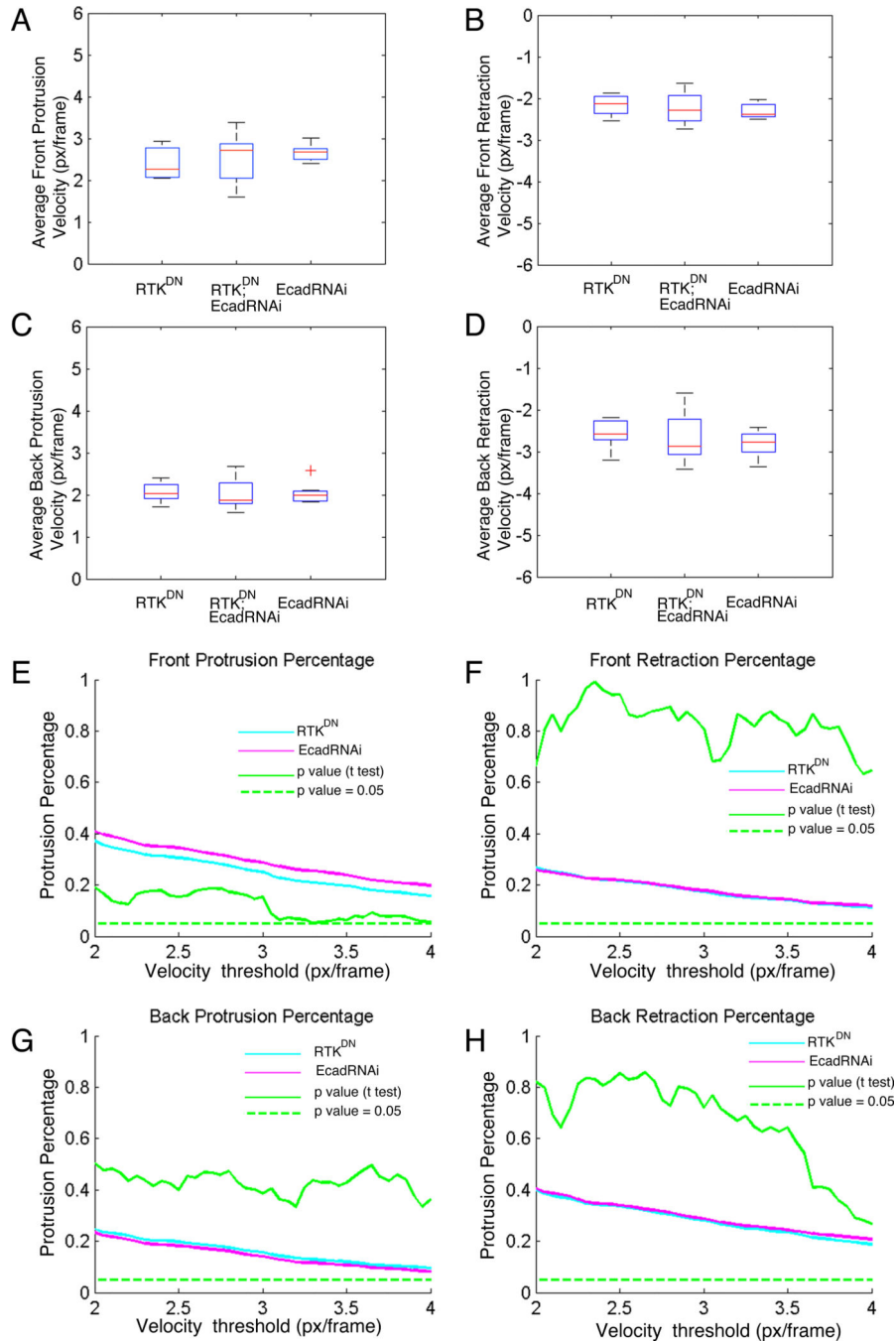
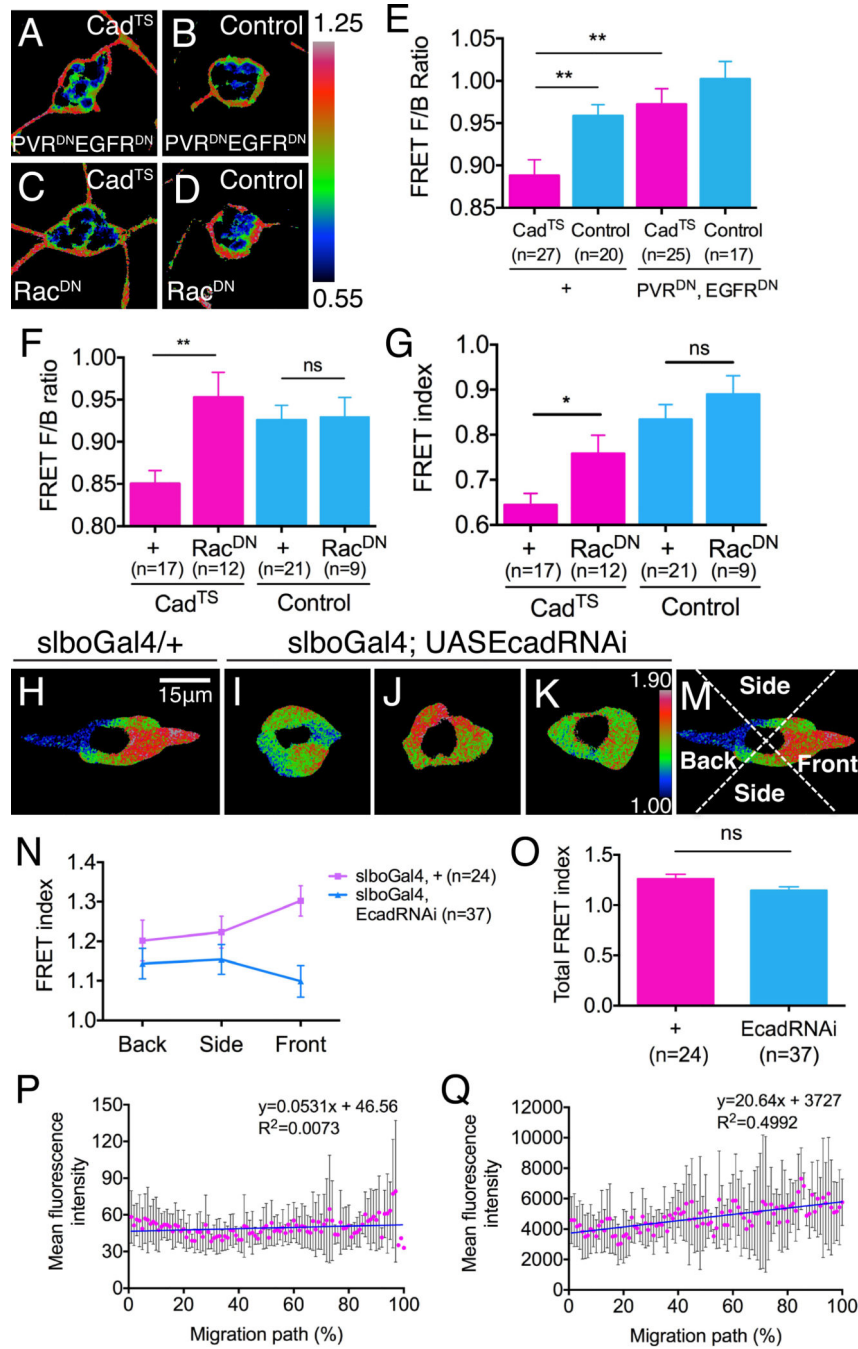


Figure 5. Border cell clusters deficient in expression of E-cadherin exhibit morphodynamic shifts identical to border cell clusters expressing dominant negative guidance receptors

(A-D) Comparison of average velocity of protruding and retracting segments at the cluster front and cluster back between border cell clusters expressing RTK^{DN} alone, or in combination with E-cadherin knock-down, and border cell clusters with E-cadherin knock-down only. (E-H) Comparison of fractions of protruding and retracting sectors at cluster front and back between border cell clusters expressing RTK^{DN} and E-cadherin knock-down. Fractional features depend on the selection of a threshold separating quiescent from protruding/retracting segments. The similarity between the features for the two genotypes is

robust across the entire range of velocity thresholds. P-values of randomization test indicated in green, on the same axis as the fractions. See also Supplemental Figure S4.



presented as mean \pm SEM. (H-K) Distribution of Rac activity in (H) a WT cluster and (I-K) three examples of clusters expressing EcadRNAi specifically in outer migratory border cells. Rac FRET images are pseudo-colored using Rainbow RGB. (M) To quantify the spatial distributions, FRET images were divided into quadrants (front, sides, back) and the mean FRET value of each quadrant determined. (N) Graph of the mean Rac FRET values for the front, sides and back of the indicated numbers of border cell clusters. Data are presented as mean \pm SEM. (O) Histogram of total FRET indices in slboGal4 egg chambers with (blue) and without (pink) EcadRNAi. Data are presented as mean \pm SEM. (P, Q) Distributions of PVF1 and E-cadherin along the border cell migration path. (P) Anti-PVF1 staining intensity and (Q) Anti-E-cadherin staining intensity along the border cell migration paths measured in stage 9 egg chambers. 0% indicates the anterior end of the egg chamber. 100% indicates the nurse cell/oocyte border. Data are presented as mean \pm SD. Linear regression was performed and line fitted to the graph.

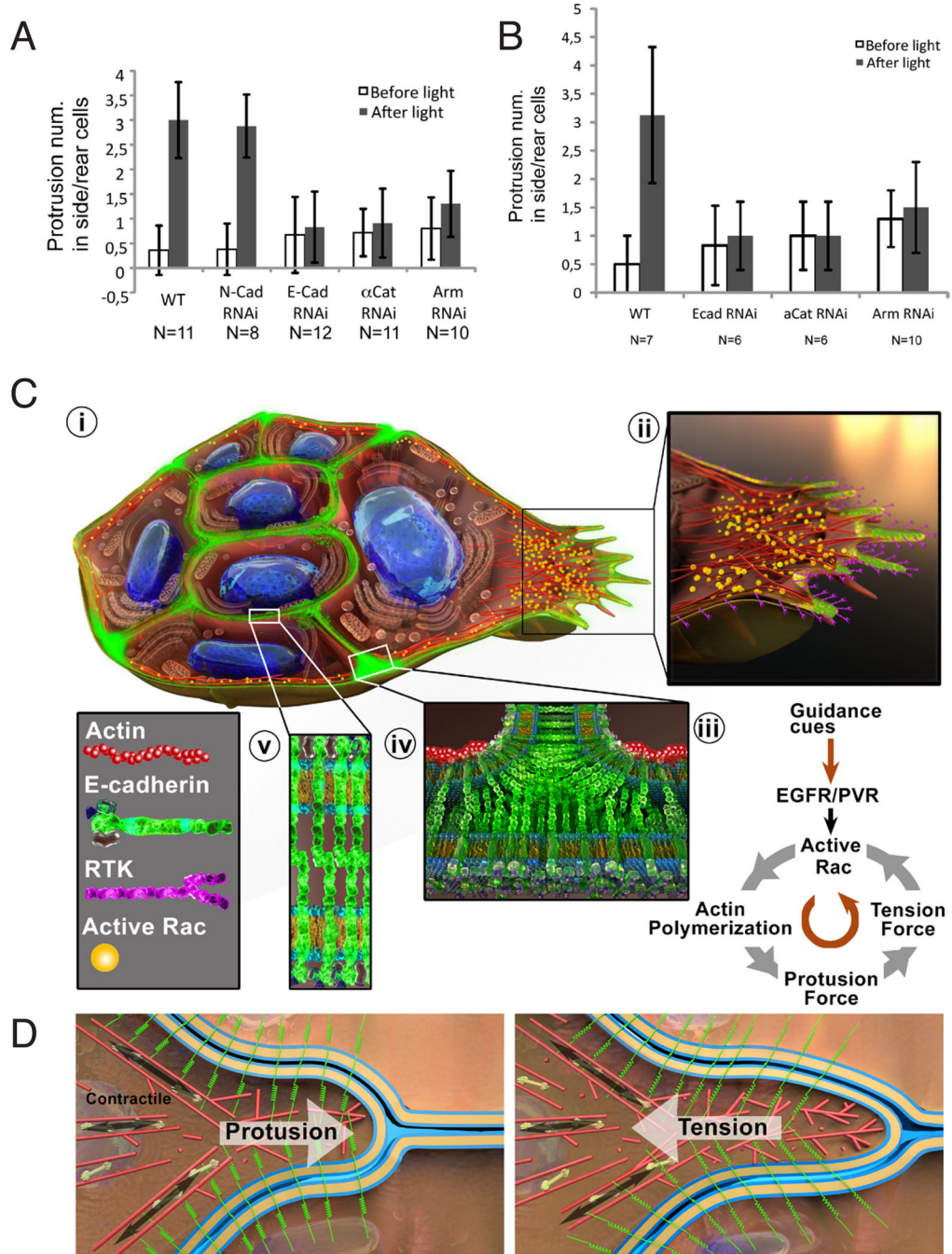


Figure 7. Adherens junction components are required for communication between border cells
 (A) Quantification of side and rear protrusions before and after photo-inactivation of Rac in the leading cell. In WT clusters and those expressing a control RNAi against N-cadherin (N-Cad) inhibition of Rac in the lead cell, using a photo-inhibitavable form of Rac, induces ectopic protrusions in other cells (Wang et al., 2010). Inhibiting expression of E-cadherin (E-cad), alpha-catenin (α Cat) or Armadillo (Arm) eliminates cell-cell communication and thus ectopic protrusions. Data are presented as mean \pm SD. (B) Photo-inhibition of Rac in flip-out clone before and after adherens junction component knock-down in the same clone.

See also Supplemental Figure S5. (C) Illustration of the multiple roles of E-cadherin in a border cell cluster migrating from left to right. i. Cutaway overview showing a central pair of polar cells surrounded by multiple migratory cells. The leading cell is on the right. ii. Enlargement of the leading edge. iii. Depiction of the feedback loop between the RTKs, E-cadherin and Rac. iv. Enlargement of a border cell-border cell junction where the high concentration of E-cadherin and coupling to F-actin cables mediate communication of direction from the lead cell to the followers. v. Enlargement of a border cell-polar cell junction where stable adhesion holds the cluster together and creates a “back” for each cell. (D) Illustration of the protrusive and contractile forces (i) that together generate tension (ii) on E-cadherin at the protruding leading edge. Actin filaments are shown in red. E-cadherin is green. Border cell and nurse cell plasma membranes are in gold.